European Journal of Medicinal Chemistry 64 (2013) 401–409

Contents lists available at SciVerse ScienceDirect

European Journal of Medicinal Chemistry

journal homepage: http://www.elsevier.com/locate/ejmech

Original article

Synthesis and antiproliferative activity of 4-substituted-piperazine-1-carbodithioate derivatives of 2,4-diaminoquinazoline

Sheng-Li Cao [a,b,*], Ying Han [a], Chong-Zhen Yuan [b,c], Yao Wang [a,b], Zhi-Kai Xiahou [b,c], Ji Liao [b,c], Rui-Ting Gao [a], Bei-Bei Mao [a,b], Bao-Li Zhao [a], Zhong-Feng Li [a], Xingzhi Xu [b,c,**]

[a] Department of Chemistry, Capital Normal University, Beijing 100048, PR China
[b] Beijing Key Laboratory of DNA Damage Response, Capital Normal University, Beijing 100048, PR China
[c] College of Life Science, Capital Normal University, Beijing 100048, PR China

ARTICLE INFO

Article history:
Received 28 February 2012
Received in revised form
3 April 2013
Accepted 8 April 2013
Available online 15 April 2013

Keywords:
2,4-Diaminoquinazoline
Piperazine-1-carbodithioate
Synthesis
Antiproliferative activity
DNA damage

ABSTRACT

A novel series of 4-substituted-piperazine-1-carbodithioate derivatives of 2,4-diaminoquinazoline were synthesized and tested for their antiproliferative activities against five human cancer cell lines including A549 (lung cancer), MCF-7 (breast adenocarcinoma), HeLa (cervical carcinoma), HT29 and HCT-116 (colorectal cancer). Most of the synthesized compounds showed broad spectrum antiproliferative activity (IC_{50} 1.47–11.83 μM), of which **8f**, **8m** and **8q** were the most active members with IC_{50} values in the range of 1.58–2.27, 1.84–3.27 and 1.47–4.68 μM against five cancer cell lines examined, respectively. Further investigations revealed that compounds **8f**, **8m** and **8q** exhibited weak inhibition against dihydrofolate reductase and no activity against thymidylate synthase, while induced DNA damage and activated the G2/M checkpoint in HCT-116 cells.

1. Introduction

Classical antifolates containing 2-methyl-4-oxoquinazoline moiety such as Raltitrexed (Fig. 1), or nonclassical antifolates containing 2-amino-4-oxoquinazoline moiety such as AG337 (Fig. 1) present anticancer potency through inhibiting thymidylate synthase [1–5]. While compounds containing 2,4-diaminopyrimidine structure, for example, Methotrexate and Trimetrexate (Fig. 1) act as anticancer drugs through targeting at dihydrofolate reductase [6–8].

DNA damage occurs at a very high frequency in our body due to assailants from endogenous factors (e.g., free radicals during metabolism) and environmental factors (e.g., ultraviolet radiation in the sunlight). Luckily, we have evolved to develop a complex, yet highly efficient DNA damage response (DDR) network to fix damaged DNA [9]. The DDR network senses damaged DNA, amplifies damage signal, and transduces it to down-stream effectors. This leads to the activation of checkpoints (G1/S, intra-S-phase, and G2/M checkpoint) to halt the cell cycle progression and allow time for repair. Among many types of DNA damage, DNA double strand break (DSB) is the most dexterous since one unrepaired DSB is sufficient to induce cell death. On the other hand, radiotherapeutic approaches and many chemotherapeutic agents, such as the topoisomerase inhibitor Camptothecin (CPT), the DNA intercalating drug Adriamycin, and the ionizing radiation-mimetic chemical, target at the cellular genomic DNA and cause DNA damage, hoping to induce cell death. Thus, developing novel DNA damaging agents is one of the trends of anti-cancer drug research.

In our previous work, a dithiocarbamate moiety that has been recognized as an anticancer pharmacophore [10–14] was incorporated into the C6 position of 2-methyl-4-oxoquinazoline to generate a number of pharmacophore hybrids [15–17]. Among them, 2-methyl-4-oxoquinazoline derivatives bearing piperazine-1-carbodithioate side chains, for instance, compound **I** (Fig. 1) exhibited significant cytotoxic activity against human leukemia K562 cells [15]. Therefore, the aim of this work was to incorporate

Abbreviations: CPT, campothecin; DDR, DNA damage response; 5-FU, 5-Fluorouracil; MTT, 3-(4,5-dimethylthiazol-2-yl)-2,5-diphenyltetrazolium bromide; MTX, Methotrexate; RTX, Raltitrexed.

* Corresponding author. Department of Chemistry, Capital Normal University, Beijing 100048, PR China. Tel./fax: +86 10 68902974.
** Corresponding author. Beijing Key Laboratory of DNA Damage Response, Capital Normal University, Beijing 100048, PR China. Tel./fax: +86 10 68902240.
E-mail addresses: slcao@cnu.edu.cn, sl_cao@163.com (S.-L. Cao), xingzhi_xu@mail.cnu.edu.cn (X. Xu).

0223-5234/$ – see front matter © 2013 Elsevier Masson SAS. All rights reserved.
http://dx.doi.org/10.1016/j.ejmech.2013.04.017

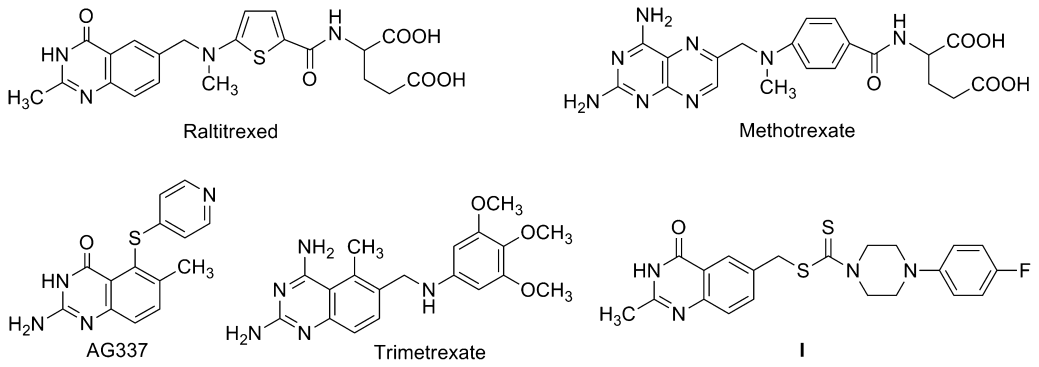

Fig. 1. Structures of Raltitrexed, Methotrexate, AG337, Trimetrexate and compound **I**.

the piperazine-1-carbodithioate moiety into the C6 position of 2,4-diaminoquinazoline to generate a novel series of compounds **8a**–**u** (Scheme 1 and Table 1), which would be investigated for their antitumour activity and possible mechanisms of antifolate or DNA damage-inducing agents.

2. Chemistry

As depicted in Scheme 1, 5-methylisatin (**1**) reacted with hydroxylamine hydrochloride to form oxime **2** [18], which was treated with sodium carbonate in *N*,*N*-dimethylformamide (DMF) to yield 2-amino-5-methylbenzonitrile (**3**) [19]. Reaction of **3** with cyanoguanidine in the presence of 1 mol/L hydrochloric acid generated the cyclized product, 2,4-diamino-6-methylquinazoline (**4**) [20], which was converted into 2,4-bis(pivaloylamino)-6-methylquinazoline (**5**) through acylation with pivaloyl chloride. Two pivaloyl groups introduced could protect the amino groups as well as enhance the solubility of compound **5** in tetrachloromethane, the solvent commonly used for bromination. Consequently, 2,4-bis(pivaloylamino)-6-(bromomethyl)quinazoline (**6**) was obtained by bromination of **5** with *N*-bromosuccinimide (NBS) in good yield. Pivaloyl groups of compound **6** were removed under acidic condition to afford 6-(bromomethyl)-2,4-diaminoquinazoline (**7**), which reacted with carbon disulfide, potassium phosphate and different 1-substituted piperazines to give target compounds **8a**–**u**.

3. Pharmacology

The MTT [3-(4,5-dimethylthiazol-2-yl)-2,5-diphenyltetrazolium bromide] cell proliferation assay was used to evaluate antiproliferative activity of the synthesized compounds against five human tumour cell lines including A549 (lung cancer), MCF-7 (breast adenocarcinoma), HeLa (cervical carcinoma), HT29 and HCT-116 (colorectal cancer). The inhibition of cell proliferation was determined 72 h after cells were exposed to the tested compounds at a concentration of 20 μM. The compounds with 50% or more inhibition compared with vehicle-treated cells were considered active. Inhibition of cell proliferation by these active compounds at various concentrations were further measured, and their IC_{50} (the concentration that causes 50% of cell proliferation inhibition) values were determined and summarized in Table 1. 5-Fluorouracil (5-FU) was used as a positive control.

Among the tested compounds, **8f**, **8m** and **8q** presented prominent activity against the proliferation of five cell lines with IC_{50} values in the range of 1.58–2.27, 1.84–3.27 and 1.47–4.68 μM, respectively. To gain further insight into the mechanisms of action of these new and active compounds, we determined if these compounds would inhibit enzymatic activities of DHFR and/or TS. In the *in vitro* enzymatic assays, we found that **8f**, **8m** and **8q** only weakly inhibited DHFR activity and TS activity (Tables 2 and 3), in comparison to the positive control compounds MTX and RTX, respectively. We further examined if treatment with these compounds in HCT-116 cells would lead to cell cycle arrest and DNA damage. HCT-116 cells were treated with **8f**, **8m** and **8q**, or 5-FU at a concentration equivalent to its IC_{50} for 24 h. Cells were harvested for cell cycle analysis by a flow cytometry. Three independent experiments were performed, and data from one representative experiment were shown in Table 4 and Fig. 2. Meanwhile, indirect immunofluorescence assay using antibody specific for the DSB marker γ-H2AX was performed to examine whether these compounds would induce DSBs in cultured cancer cells, and the results

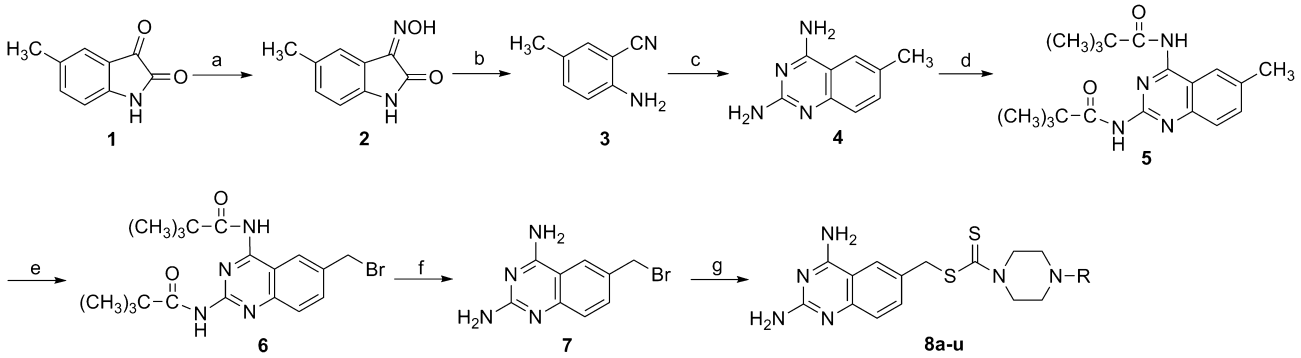

Scheme 1. Synthetic route to compounds **8a**–**u**. Reagents and conditions: a. $NH_2OH{\cdot}HCl/H_2O$, reflux, 40 min; b. Na_2CO_3, DMF, 125–135 °C, 2.5 h; c. $H_2NC(=NH)NHCN$, HCl/H_2O, reflux, 1.5 h; d. $(CH_3)_3CCOCl$, Et_3N, 1,4-dioxane, reflux, 30 min; e. NBS, $(PhCO)_2O_2$, CCl_4, reflux, 10 h; f. HCl/MeOH, reflux, 4 h; g. 1-substituted piperazines, CS_2, K_3PO_4, DMF, r.t., 4 h.

Table 1
Antiproliferative activity (IC_{50}, μM) of compounds **8a**–**u** against five human cancer cell lines.

No.	R	IC_{50}[a], μM				
		A549	MCF-7	HeLa	HT29	HCT-116
8a	CH_3	9.20 ± 0.42	>20[b]	>20	>20	>20
8b	Cyclohexyl	4.71 ± 0.30	6.80 ± 0.11	5.96 ± 0.33	4.05 ± 0.09	8.40 ± 0.06
8c	$C_6H_5CH_2$	3.31 ± 0.48	8.46 ± 0.75	8.35 ± 0.11	8.49 ± 1.01	4.91 ± 0.69
8d	C_6H_5	2.97 ± 0.33	2.95 ± 0.57	2.84 ± 0.40	2.76 ± 0.42	4.12 ± 0.10
8e	4-HOC_6H_4	4.21 ± 0.09	5.09 ± 0.57	5.18 ± 0.92	>20	5.98 ± 0.83
8f	4-$CH_3OC_6H_4$	1.59 ± 0.02	1.58 ± 0.04	1.66 ± 0.33	1.77 ± 0.17	2.27 ± 0.23
8g	4-$CH_3C_6H_4$	2.19 ± 0.43	2.48 ± 0.19	2.13 ± 0.05	3.02 ± 0.06	5.51 ± 0.37
8h	2-$CH_3C_6H_4$	3.92 ± 0.54	4.23 ± 0.03	n.d.[c]	2.95 ± 0.07	11.83 ± 0.19
8i	2,4-di$CH_3C_6H_3$	3.00 ± 0.13	3.12 ± 0.03	3.19 ± 0.07	2.97 ± 0.06	4.07 ± 0.05
8j	4-ClC_6H_4	5.21 ± 0.10	4.88 ± 0.36	6.99 ± 0.58	7.48 ± 0.47	7.38 ± 0.32
8k	2-ClC_6H_4	3.61 ± 0.31	3.19 ± 0.39	4.05 ± 0.22	3.90 ± 0.39	5.49 ± 0.89
8l	3,4-diClC_6H_3	2.94 ± 0.32	2.37 ± 0.06	3.06 ± 0.08	3.48 ± 0.32	6.68 ± 0.01
8m	4-FC_6H_4	2.04 ± 0.11	1.92 ± 0.02	1.84 ± 0.12	2.05 ± 0.22	3.27 ± 0.39
8n	2-FC_6H_4	6.46 ± 0.44	4.84 ± 0.20	6.66 ± 0.22	5.42 ± 0.85	n.d.
8o	2,4-diFC_6H_3	5.12 ± 0.31	3.67 ± 0.62	3.80 ± 0.34	5.02 ± 0.34	5.15 ± 0.16
8p	4-$CH_3COC_6H_4$	2.55 ± 0.16	2.49 ± 0.11	2.04 ± 0.02	2.28 ± 0.13	8.26 ± 0.10
8q	4-$NO_2C_6H_4$	1.91 ± 0.06	1.47 ± 0.16	1.66 ± 0.52	3.32 ± 0.26	4.68 ± 0.87
8r	2-$NO_2C_6H_4$	4.36 ± 0.61	4.35 ± 0.2	4.88 ± 0.44	4.31 ± 0.23	5.52 ± 1.60
8s	4-$CF_3C_6H_4$	>20	7.40 ± 1.74	>20	>20	>20
8t	2-Pyridinyl	3.96 ± 0.19	5.11 ± 0.23	5.09 ± 0.07	6.20 ± 0.76	5.96 ± 0.07
8u	2-Pyrimidinyl	4.01 ± 0.01	4.19 ± 0.49	4.36 ± 0.08	4.72 ± 0.52	5.84 ± 0.03
5-FU		3.52 ± 0.46	32.18 ± 1.13	43.71 ± 3.49	24.50 ± 2.62	5.53 ± 0.90

[a] IC_{50}: The concentration that causes 50% of cell proliferation inhibition. Data are expressed as means ± SD of at least three separate experiments.
[b] IC_{50} > 20 μM indicates that cell growth inhibition is lower than 50% at the concentration of 20 μM.
[c] n.d.: Compound inhibited cell growth by 50% or more but the IC_{50} value was not determined.

were demonstrated in Fig. 3, and mitotic index was determined to assess the activation of the G2/M checkpoint and the results were illustrated in Table 5 and Fig. 4.

4. Results and discussion

4.1. Antiproliferative activity

To search for more efficient anticancer agents and to investigate the structure–activity relationship of 4-substituted-piperazine-1-carbodithioate derivatives of 2,4-diaminoquinazoline, methyl, cyclohexyl, benzyl, phenyl, as well as pyridin-2-yl and pyrimidin-2-yl groups were selected to serve as R substituents in the target compounds (Scheme 1). Particularly, a number of substituted phenyl groups were incorporated into compounds **8e**–**s** to examine the electronic or steric effects of substituents attached to the phenyl ring on the antiproliferative activity. All the target compounds were screened for their antiproliferative activities against a panel of five human tumour cell lines: A549, MCF-7, HeLa, HT29 and HCT-116. It can be seen from Table 1 that most compounds except **8a** and **8s** showed broad spectrum antitumour activity against the five cell lines tested. In comparison with compounds **8a**–**c**, **8d** exhibited higher antiproliferative activity against all five cancer cell lines with IC_{50} values in the range of 2.76–4.12 μM. Furthermore, replacement of the phenyl group in **8d** with pyridin-2-yl or pyrimidin-2-yl resulted in compounds **8t** and **8u**, both of which exhibited a

Table 2
Inhibitory activity of compounds **8f**, **8m** and **8q** against human dihydrofolate reductase.

Compound	IC_{50} (μM)
8f	5.96
8m	2.11
8q	1.61
MTX	0.0021

Table 3
Percent inhibition of compounds **8f**, **8m** and **8q** against human thymidylate synthase.

Compound	Concentration (μM)	Inhibition (%)[a]
8f	50	15.22 ± 6.61
8m	50	19.94 ± 3.81
8q	50	14.08 ± 0.94
RTX	1	94.23 ± 3.23

[a] Percent inhibition values of **8f**, **8m** and **8q** against human thymidylate synthase were lower than 50% at the concentration of 50 μM, which were considered inactive and not determined for their IC_{50} values. Nevertheless, the IC_{50} value of RTX (0.26 μM) was determined by serial dilution.

Table 4
Effects of compounds **8f**, **8m** and **8q** on HCT-116 cell cycle progression.

Compound	Cell cycle distribution (%)		
	G0/G1	S	G2/M
DMSO	63.07	25.39	11.54
5-FU	45.44	47.75	6.81
8f	52.36	33.34	14.29
8m	46.63	39.22	14.15
8q	44.74	39.46	15.80

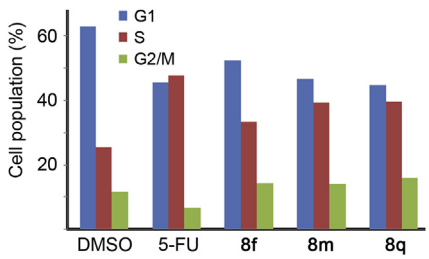

Fig. 2. Effects of compounds **8f**, **8m** and **8q** on cell cycle distribution. HCT-116 cells were treated with **8f**, **8m** and **8q**, or 5-Fluorouracil (C) at the concentration equivalent to their IC_{50} for 24 h.

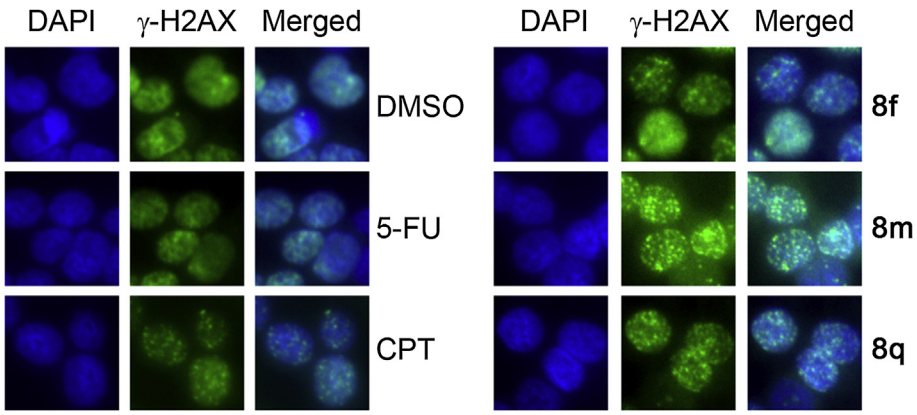

Fig. 3. Treatment of HCT-116 cells with **8f**, **8m** or **8q** for 2 h induced formation of γ-H2AX foci.

decrease in antiproliferative activity against five cell lines. These results indicate that an aryl group connected to the N4 position of piperazine ring is more favourable for antiproliferative activity than an alkyl, cycloalkyl, arylalkyl or heteroaryl group. Among the compounds bearing an aryl group at the N4 position of piperazine ring, **8f**, **8m** and **8q** were the most active members with IC_{50} values of 1.58–2.27, 1.84–3.27 and 1.47–4.68 μM against the five cell lines, respectively, which were more potent than the clinically used anticancer drug 5-FU. Previously, we reported the synthesis of 2-methyl-4-oxoquinazoline derivatives bearing piperazine-1-carbodithioate side chains together with their cytotoxicity against human leukemia K562 cell line [15]. From a few compounds examined, it still could be seen that the cytotoxic activity enhanced as the substituent at the N4 position of piperazine varied from methyl, benzyl to 4-fluorophenyl. This structure–activity trend is generally in common with the above-mentioned observation from the present work. Moreover, similar to the most potent compound **I** in 2-methyl-4-oxoquinazoline series (Fig. 1), **8m** containing the same 4-fluorophenypiperazine-1-carbodithioate moiety was one of the most potent compounds derived from 2,4-diaminoquinazoline.

As shown in Table 1, introduction of either an electron-donating substituent (4-CH_3O, **8f**) or an electron-withdrawing substituent (4-F, **8m**) at the 4-position of the benzene ring in **8d** led to an increase in activity against each cell line in comparison with the counterpart **8d**. Similarly, compounds **8g** (4-CH_3), **8p** (4-CH_3CO) and **8q** (4-NO_2) exhibited higher activity against A549, MCF-7 and HeLa cell lines than the parent compound **8d**. However, an obvious decrease in antiproliferative activity against five cell lines was observed when the methoxyl (**8f**), methyl (**8g**), or fluorine atom (**8m**) were converted to hydroxyl (**8e**), trifluoromethyl (**8s**) or chlorine (**8j**), respectively. These results suggest that both the electronic and steric effects of the substituents at the 4-position of benzene rings play important roles in generating the antiproliferative activity. On the other hand, compound **8g** (4-CH_3), **8m** (4-F) and **8q** (4-NO_2) showed higher activity than the counterparts **8h** (2-CH_3), **8n** (2-F) and **8r** (2-NO_2), respectively, with the exception of **8j** (4-Cl) versus **8k** (2-Cl). Moreover, further introduction of a methyl group at the 2-position of **8g** (4-CH_3) or a fluorine atom at 2-position of **8m** (4-F) resulted in **8i** (2,4-diCH_3) and **8o** (2,4-diF). **8i** and **8o** exhibited slightly decreased activity in comparison with the parent compounds **8g** (4-CH_3) and **8m** (4-F), whereas they showed increased activity over the 2-substituted counterparts **8h** (2-CH_3) and **8n** (2-F). However, introduction of a chlorine atom at the 3-position of **8j** (4-Cl) resulted in **8l** (3,4-diCl), which displayed higher activity than either the 4- or 2-*mono*-substituted counterparts (**8j**, 4-Cl; **8k**, 2-Cl). Taken together, the presence of a substituent at the 4-position of benzene ring is a critical determinant of activity, while the electronic and steric characters of the substituents are less important for activity.

4.2. Effects of compounds *8f*, *8m* and *8q* on DHFR and TS

Since compounds **8f**, **8m** and **8q** were derived from antifolate agents, we sought to determine if they would inhibit the enzymatic activities of DHFR and/or TS. In the *in vitro* DHFR inhibition assays, MTX at the concentration of 5 nM reduced about 86% of DHFR activity, and achieved an IC_{50} of 2 nM. However, compounds **8f**, **8m** and **8q** at the concentration of 500 nM only reduced 24%, 35%, and 29% of DHFR activity with an IC_{50} of 5.96 μM, 2.11 μM, and 1.61 μM, respectively (Table 2). Similarly, in the *in vitro* TS assays, RTX at the concentration of 1 μM reduced about 94% of TS activity, whereas **8f**, **8m** and **8q** at the concentration of 50 μM only reduced about 14–20% of TS activity (Table 3). These results suggest that compounds **8f**, **8m** and **8q** weakly inhibit DHFR activity, while exhibit essentially no activity against TS. Thus, these compounds are not potent antifolate agents.

Table 5
Mitotic indexes of HCT-116 cells treated with compounds **8f**, **8m** and **8q** for 2 h.

Compound	Mitotic index
DMSO	0.98
CPT	0.64
8f	0.76
8m	0.45
8q	0.67

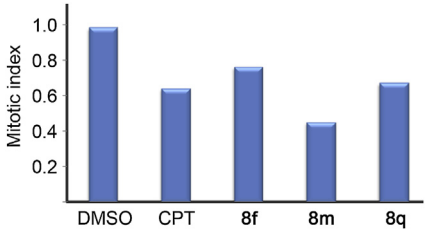

Fig. 4. Treatment of HCT-116 cells with CPT, **8f**, **8m** or **8q** for 2 h activated the G2/M checkpoint.

4.3. Effects of compounds **8f**, **8m** and **8q** on the cell cycle progression and DNA damage response in cells

An antifolate agent blocks DNA synthesis, leading to the cell cycle arrest at the early S phase. We thus sought to determine if these compounds would have an impact on the cell cycle progression. When HCT-116 cells were treated with 5-FU for 24 h, S-phase cells were accumulated as expected, whereas treatment with **8f**, **8m** or **8q** resulted in a slight increase of S-phase cells and a significant increase of G2/M cells (Table 4 and Fig. 2). This suggests that these compounds, like many chemotherapeutic agents that cause DNA damage, induce G2/M arrest in cancer cells. We thus reasoned if these compounds would induce DNA damage in cultured cancer cells. Indeed, the DSB marker, Ser-139 phosphorylated form of H2AX (γ-H2AX) did not form discrete nuclear foci in HCT-116 cells treated with 5-FU for 2 h, whereas treatment with CPT, **8f**, **8m**, or **8q** for 2 h induced γ-H2AX focus formation (Fig. 3) and resulted in an obvious reduction of the mitotic index (Table 5 and Fig. 4). CPT is a known topoisomerase inhibitor and DNA damage inducer. These data demonstrate that compounds **8f**, **8m** and **8q** induce DNA damage in HCT-116 cells, leading to the G2/M arrest and the G2/M checkpoint activation. Given the fact that most antifolate agents induce a cell cycle arrest at S phase [21] and do not lead to obvious damage to the genomic DNA in cells, whereas most DNA damage-based chemotherapeutic agents induce a cell cycle arrest at G2/M phase and activate the G2/M checkpoint to allow time for cells to fix the damaged DNA [9]. Therefore, we believe that the molecular targets of compounds **8f**, **8m** and **8q**, in addition to DHFR and TS, include DDR factors, which is under investigation in our laboratories.

5. Conclusion

A set of 4-substituted-piperazine-1-carbodithioate derivatives of 2,4-diaminoquinazoline were synthesized and most of them showed broad spectrum inhibitory effects on the proliferation of five human tumour cell lines including A549, MCF-7, HeLa, HT29 and HCT-116 cell lines. Analysis of structure–activity relationship indicates that a phenyl group connected to the N4 position of piperazine ring is more favorable for the antiproliferative activity than a methyl, cyclohexyl, benzyl, pyridin-2-yl or pyrimidin-2-yl group. Furthermore, some compounds bearing substituents such as methoxyl, methyl, nitro group and fluorine atom at the 4-position of the phenyl ring exhibited higher activity than the unsubstituted counterpart, whereas analogues bearing substituents like methyl, nitro group and fluorine atom at the 2-position of the phenyl ring showed lower activity than the parent compound. These results reveal that the electronic effect of substituents is not a critical determinant of activity, whereas the position or steric effect of substituents exerts remarkable influence on the antiproliferative activity. Furthermore, different from 5-FU, compounds **8f**, **8m** and **8q** induced DNA damage in HCT-116 cells, leading to the G2/M checkpoint activation and G2/M arrest.

6. Experimental

6.1. Chemistry

Melting points were determined on an X-6 microscopic melting point apparatus and are uncorrected. ^{1}H NMR spectra were recorded on a Bruker AC-200P spectrometer at 200 MHz, or a Varian Plus 300 spectrometer at 300 MHz, or a Varian VNMRS-600 spectrometer at 600 MHz using tetramethylsilane (TMS) as internal standard. Electron impact (EI) mass spectra were recorded on a Shimadzu GCMS-QP2010 Plus mass spectrometer. Low-resolution electrospray ionization (ESI) mass spectra were recorded on a Bruker Daltonics Esquire-LC 00136 mass spectrometer or a Waters UPLC/Q-Tof Micro mass spectrometer, and high-resolution electrospray ionization (HR-ESI) mass spectra were recorded on an Agilent LC/SMD TOF mass spectrometer. Elemental analyses were performed by Institute of Chemistry, Chinese Academy of Science, on a Flash EA 1112 elemental analyzer. Column chromatography was carried out on silica gel (200–300 mesh).

6.1.1. Preparation of 3-(hydroxyimino)-5-methylindolin-2-one (**2**)

A mixture of 5-methylindoline-2,3-dione (**1**) (2.2 g, 13.6 mmol), hydroxylamine hydrochloride (1.1 g, 15.8 mmol) and water (15 mL) was refluxed for 40 min. After cooling to room temperature, the precipitate was collected by filtration, washed with water and dried in air to give 2.2 g (92%) of **2**, mp 202.0–204.7 °C (Lit. [22] mp 202–204 °C). ^{1}H NMR (600 MHz, DMSO-d_6) δ: 2.26 (s, 3H, CH_3), 6.76 (d, $J = 7.8$ Hz, 1H, indolin-2-one 7-H), 7.16 (d, $J = 7.8$ Hz, 1H, indolin-2-one 6-H), 7.78 (s, 1H, indolin-2-one 4-H), 10.56 (s, 1H, OH), 13.23 (s, 1H, NH). EI-MS m/z: 176 $[M]^+$.

6.1.2. Preparation of 2-amino-5-methylbenzonitrile (**3**)

A solution of 3-(hydroxyimino)-5-methylindolin-2-one (**2**) (1.76 g, 10 mmol) and sodium carbonate (0.1 g, 0.9 mmol) in *N*,*N*-dimethylformamide (5 mL) was heated at 125–135 °C for 2.5 h. After cooling to room temperature, water (20 mL) was added and the solution was extracted with ethyl acetate (20 mL × 3). The combined organic phases were washed with saturated saline solution and dried over anhydrous Na_2SO_4 overnight. The solvent was removed by rotary evaporation and the residue was purified by column chromatography using petroleum ether/ethyl acetate (4:1) as an eluent to give 1.13 g (85%) of **3** as a yellowish solid, mp 60.5–61.0 °C (Lit. [17] mp 59–60 °C). ^{1}H NMR (600 MHz, $CDCl_3$) δ: 2.33 (s, 3H, CH_3), 4.25 (br s, 2H, NH_2), 6.66 (d, $J = 8.4$ Hz, 1H, 3-H), 7.14 (d, $J = 8.4$ Hz, 1H, 4-H), 7.18 (s, 1H, 6-H). EI-MS m/z: 132 $[M]^+$.

6.1.3. Preparation of 2,4-diamino-6-methylquinazoline (**4**)

A mixture of 2-amino-5-methylbenzonitrile (**3**) (0.7 g, 5.3 mmol), cyanoguanidine (0.45 g, 5.3 mmol) and 1 mol/L hydrochloric acid (5 mL) was heated under reflux for 1.5 h. The mixture was diluted with water (13 mL) and 1 mol/L hydrochloric acid (5 mL), and heated for a while. The hot solution was filtered, and then 2 mol/L sodium hydroxide solution (11 mL) was added into the filtrate. The yellow solid formed was collected by filtration and dried in air. The solid was mixed with water (8 mL) and 88% formic acid (2 mL), the mixture was stirred until the yellow solid converted into white solid. The solid was filtered off and dissolved in water (25 mL), and the solution was adjusted to strongly basic with aqueous ammonia solution. The separated solid was collected by filtration and dried to yield 0.43 g (48%) of **4** as a yellow solid, mp 258.8–259.4 °C (Lit. [19] mp 258–259.5 °C). ^{1}H NMR (600 MHz, DMSO-d_6) δ: 2.33 (s, 3H, CH_3), 5.85 (br s, 2H, NH_2), 7.11 (d, $J = 8.4$ Hz, 1H, quinazoline 8-H), 7.15 (br s, 2H, NH_2), 7.32 (d, $J = 8.4$ Hz, 1H, quinazoline 7-H), 7.76 (s, 1H, quinazoline 5-H). ESI-MS m/z: 175 $[M + H]^+$.

6.1.4. Preparation of 2,4-bis(pivaloylamino)-6-methylquinazoline (**5**)

To a boiling solution of 2,4-diamino-6-methylquinazoline (**4**) (2.1 g, 12.1 mmol), triethylamine (5 mL, 35 mmol) and 1,4-dioxane (22 mL) was added pivaloyl chloride (4.2 g, 35 mmol) in 1,4-dioxane (5.5 mL). After refluxing for 30 min, the mixture was filtered while it was hot, and the solid was washed several times with hot 1,4-dioxane. After cooling to room temperature, the separated solid was filtered off and washed with 1,4-dioxane. The filtrate was evaporated under reduced pressure, and the residue was purified by recrystallization from acetone to give 2.3 g (54%) of **5** as a white solid, mp 192.7–193.8 °C. ^{1}H NMR (200 MHz, DMSO-d_6) δ: 1.26 (s, 9H, $C(CH_3)_3$), 1.27 (s, 9H, $C(CH_3)_3$), 2.45 (s, 3H, CH_3), 7.43 (d,

J = 8.3 Hz, 1H, quinazoline 8-H), 7.56 (s, 1H, NH), 7.66 (d, J = 8.3 Hz, 1H, quinazoline 7-H), 7.76 (s, 1H, NH), 8.19 (s, 1H, quinazoline 5-H). ESI-MS m/z: 343 $[M + H]^+$. Anal. calcd. for $C_{19}H_{26}N_4O_2$: C, 66.64; H, 7.65; N, 16.36. Found: C, 66.65; H, 7.66; N, 16.33.

*6.1.5. Preparation of 2,4-bis(pivaloylamino)-6-(bromomethyl) quinazoline (**6**)*

A solution of 2,4-bis(pivaloylamino)-6-methylquinazoline (**5**) (1.6 g, 4.7 mmol), *N*-bromosuccinimide (NBS) (0.88 g, 4.9 mmol), benzoyl peroxide (25 mg, 0.1 mmol) in tetrachloromethane (40 mL) was refluxed for 10 h. The solvent was removed by rotary evaporation and the residue was recrystallized from cyclohexane to yield 1.5 g (74%) of **6** as a white solid, mp 114.5–115.2 °C. ^{1}H NMR (200 MHz, $CDCl_3$) δ: 1.35 (s, 9H, $C(CH_3)_3$), 1.36 (s, 9H, $C(CH_3)_3$), 4.62 (s, 2H, CH_2Br), 7.45 (d, J = 8.4 Hz, 1H, quinazoline 8-H), 7.76 (d, J = 8.4 Hz, 1H, quinazoline 7-H), 8.46 (s, 1H, quinazoline 5-H), 8.66 (br s, 1H, NH), 9.13 (br s, 1H, NH). ESI-MS m/z: 443, 445 $[M + Na]^+$. Anal. calcd. for $C_{19}H_{25}BrN_4O_2 \cdot 1/2H_2O$: C, 53.03; H, 6.09; N, 13.02. Found: C, 52.63; H, 6.03; N, 12.75.

*6.1.6. Preparation of 6-(bromomethyl)-2,4-diaminoquinazoline (**7**)*

To a warmed suspension of 2,4-bis(pivaloylamino)-6-(bromomethyl)quinazoline (**6**) (2 g, 4.8 mmol) in tetrahydrofuran (10 mL), a saturated methanolic solution of hydrogen chloride (10 mL) was added dropwise. After the solid was completely dissolved, water (2 mL) was added and the reaction mixture was heated under reflux for 4 h. The solvent was removed by rotary evaporation, and the residue was washed with acetone, filtered and dried to give 1.06 g (88%) of **7** as a white solid, mp > 300 °C. ^{1}H NMR (600 MHz, DMSO-d_6) δ: 4.41 (s, 2H, CH_2Br), 6.54 (s, 2H, NH_2, D_2O exchangeable), 7.26 (d, J = 8.4 Hz, 1H, quinazoline 8-H), 7.53 (d, J = 8.4 Hz, 1H, quinazoline 7-H), 7.77 (br s, 2H, NH_2, D_2O exchangeable), 8.03 (s, 1H, quinazoline 5-H). ESI-HRMS m/z: calcd for $C_9H_{10}BrN_4$ ($[M + H]^+$): 253.0089, 255.0068, found: 253.0087, 255.0050.

*6.1.7. General procedure for the preparation of compounds **8a–u***

A mixture of 1-substituted piperazines (1.5 mmol), carbon disulfide (0.45 mL, 7.5 mmol) and finely powered anhydrous potassium phosphate (0.32 g, 1.5 mmol) in DMF (7.5 mL) was stirred at room temperature for 30 min. 6-(Bromomethyl)-2,4-diaminoquinazoline (**7**) (0.38 g, 1.5 mmol) was added to the solution, and stirring was continued at room temperature for 4 h. After poured into water (100 mL), the resulting precipitate was collected by filtration, which was purified by column chromatography (CC) on silica gel or recrystallization from appropriate solvent to give compounds **8a–u**.

*6.1.7.1. (2,4-Diaminoquinazolin-6-yl)methyl 4-methylpiperazine-1-carbodithioate (**8a**).* Yield 61%, white solid, mp 237.8–239.0 °C (CC, eluent:dichloromethane/methanol = 80:20). ^{1}H NMR (200 MHz, DMSO-d_6) δ: 2.22 (s, 3H, NCH_3), 2.42 (br s, 4H, piperazine-H), 3.89 (br s, 2H, piperazine-H), 4.22 (br s, 2H, piperazine-H), 4.57 (s, 2H, CH_2S), 7.38 (d, J = 8.4 Hz, 1H, quinazoline 8-H), 7.51 (br s, 2H, NH_2), 7.76 (d, J = 8.4 Hz, 1H, quinazoline 7-H), 8.22 (s, 1H, quinazoline 5-H), 8.56 (br s, 2H, NH_2). ESI-MS m/z: 349 $[M + H]^+$. ESI-HRMS m/z: calcd for $C_{15}H_{21}N_6S_2$ ($[M + H]^+$): 349.1269, found: 349.1251.

*6.1.7.2. (2,4-Diaminoquinazolin-6-yl)methyl 4-cyclohexylpiperazine-1-carbodithioate (**8b**).* Yield 22%, white solid, mp 273.2–275.0 °C (CC, eluent:dichloromethane/methanol = 90:10). ^{1}H NMR (600 MHz, DMSO-d_6) δ: 1.05–1.20 (m, 5H, cyclohexyl-H), 1.55–1.75 (m, 5H, cyclohexyl-H), 2.27 (m, 1H, cyclohexyl-H), 2.55 (br s, 4H, piperazine-H), 3.84 (br s, 2H, piperazine-H), 4.20 (br s, 2H, piperazine-H), 4.47 (s, 2H, CH_2S), 5.99 (br s, 2H, NH_2), 7.14 (d, J = 8.4 Hz, 1H, quinazoline 8-H), 7.24 (br s, 2H, NH_2), 7.49 (d, J = 8.4 Hz, 1H, quinazoline 7-H), 7.99 (s, 1H, quinazoline 5-H). ESI-MS m/z: 417 $[M + H]^+$. ESI-HRMS m/z: calcd for $C_{20}H_{29}N_6S_2$ ($[M + H]^+$): 417.1895, found: 417.1884.

*6.1.7.3. (2,4-Diaminoquinazolin-6-yl)methyl 4-benzylpiperazine-1-carbodithioate (**8c**).* Yield 28%, white solid, mp 268.6–269.0 °C (CC, eluent:dichloromethane/methanol = 90:10). ^{1}H NMR (600 MHz, DMSO-d_6) δ: 2.44 (br s, 4H, piperazine-H), 3.51 (s, 2H, CH_2Ph), 3.88 (br s, 2H, piperazine-H), 4.22 (br s, 2H, piperazine-H), 4.55 (s, 2H, CH_2S), 7.25 (t, J = 6.6 Hz, 1H, Ph 4′-H), 7.30 (m, 4H, Ph 2′, 3′, 5′ and 6′-H), 7.38 (d, J = 8.4 Hz, 1H, quinazoline 8-H), 7.77 (d, J = 8.4 Hz, 1H, quinazoline 7-H), 8.25 (s, 1H, quinazoline 5-H). ESI-MS m/z: 425 $[M + H]^+$. ESI-HRMS m/z: calcd for $C_{21}H_{25}N_6S_2$ ($[M + H]^+$): 425.1582, found: 425.1570.

*6.1.7.4. (2,4-Diaminoquinazolin-6-yl)methyl 4-phenylpiperazine-1-carbodithioate (**8d**).* Yield 58%, white solid, mp 221.4–223.9 °C (CC, eluent:dichloromethane/methanol = 80:20). ^{1}H NMR (600 MHz, DMSO-d_6) δ: 3.28 (br s, 4H, piperazine-H), 4.04 (br s, 2H, piperazine-H), 4.39 (br s, 2H, piperazine-H), 4.51 (s, 2H, CH_2S), 6.81 (t, J = 7.8 Hz, 1H, Ph 4′-H), 6.94 (d, J = 7.8 Hz, 2H, Ph 2′ and 6′-H), 7.15 (d, J = 8.4 Hz, 1H, quinazoline 8-H), 7.23 (t, J = 7.8 Hz, 2H, Ph 3′ and 5′-H), 7.25 (br s, 2H, NH_2), 7.51 (d, J = 8.4 Hz, 1H, quinazoline 7-H), 8.01 (s, 1H, quinazoline 5-H). ESI-MS m/z: 411 $[M + H]^+$. ESI-HRMS m/z: calcd for $C_{20}H_{23}N_6S_2$ ($[M + H]^+$): 411.1426, found: 411.1420.

*6.1.7.5. (2,4-Diaminoquinazolin-6-yl)methyl 4-(4-hydroxyphenyl) piperazine-1-carbodithioate (**8e**).* Yield 27%, grey solid, mp 248.5–250.2 °C (CC, eluent:dichloromethane/methanol = 90:10). ^{1}H NMR (600 MHz, DMSO-d_6) δ: 3.04 (br s, 4H, piperazine-H), 4.0 (br s, 2H, piperazine-H), 4.34 (br s, 2H, piperazine-H), 4.52 (s, 2H, CH_2S), 6.56 (br s, 2H, NH_2), 6.65 (d, J = 9.0 Hz, 2H, Ph 2′ and 6′-H), 6.79 (d, J = 9.0 Hz, 2H, Ph 3′ and 5′-H), 7.21 (d, J = 8.4 Hz, 1H, quinazoline 8-H), 7.59 (d, J = 8.4 Hz, 1H, quinazoline 7-H), 7.74 (br s, 2H, NH_2), 8.07 (s, 1H, quinazoline 5-H), 8.91 (br s, 1H, OH). ESI-MS m/z: 427 $[M + H]^+$. ESI-HRMS m/z: calcd for $C_{20}H_{23}N_6OS_2$ ($[M + H]^+$): 427.1375, found: 427.1366.

*6.1.7.6. (2,4-Diaminoquinazolin-6-yl)methyl 4-(4-methoxyphenyl) piperazine-1-carbodithioate (**8f**).* Yield 52%, white solid, mp 238.0–239.3 °C (CC, eluent:dichloromethane/methanol = 90:10). ^{1}H NMR (600 MHz, DMSO-d_6) δ: 3.10 (br s, 4H, piperazine-H), 3.67 (s, 3H, OCH_3), 4.02 (br s, 2H, piperazine-H), 4.36 (br s, 2H, piperazine-H), 4.53 (s, 2H, CH_2S), 6.67 (br s, 2H, NH_2), 6.82 (d, J = 9.0 Hz, 2H, Ph 2′ and 6′-H), 6.90 (d, J = 9.0 Hz, 2H, Ph 3′ and 5′-H), 7.23 (d, J = 8.4 Hz, 1H, quinazoline 8-H), 7.61 (d, J = 8.4 Hz, 1H, quinazoline 7-H), 7.86 (br s, 2H, NH_2), 8.09 (s, 1H, quinazoline 5-H). ESI-MS m/z: 441 $[M + H]^+$. ESI-HRMS m/z: calcd for $C_{21}H_{25}N_6OS_2$ ($[M + H]^+$): 441.1531, found: 441.1522.

*6.1.7.7. (2,4-Diaminoquinazolin-6-yl)methyl 4-(4-methylphenyl) piperazine-1-carbodithioate (**8g**).* Yield 61%, yellowish solid, mp 227.6–230.0 °C (CC, eluent:dichloromethane/methanol = 90:10). ^{1}H NMR (600 MHz, DMSO-d_6) δ: 2.20 (s, 3H, CH_3), 3.20 (br s, 4H, piperazine-H), 4.04 (br s, 2H, piperazine-H), 4.37 (br s, 2H, piperazine-H), 4.51 (s, 2H, CH_2S), 6.0 (br s, 2H, NH_2), 6.85 (d, J = 8.4 Hz, 2H, Ph 2′ and 6′-H), 7.05 (d, J = 8.4 Hz, 2H, Ph 3′ and 5′-H), 7.15 (d, J = 8.4 Hz, 1H, quinazoline 8-H), 7.29 (br s, 2H, NH_2), 7.51 (d, J = 8.4 Hz, 1H, quinazoline 7-H), 8.05 (s, 1H, quinazoline 5-H). ESI-MS m/z: 425 $[M + H]^+$. ESI-HRMS m/z: calcd for $C_{21}H_{25}N_6S_2$ ($[M + H]^+$): 425.1582, found: 425.1572.

*6.1.7.8. (2,4-Diaminoquinazolin-6-yl)methyl 4-(2-methylphenyl) piperazine-1-carbodithioate (**8h**).* Yield 30%, yellowish solid, mp > 300 °C (CC, eluent:dichloromethane/methanol = 90:10). ^{1}H

NMR (600 MHz, DMSO-d_6) δ: 2.27 (s, 3H, CH_3), 2.91 (br s, 4H, piperazine-H), 4.03 (br s, 2H, piperazine-H), 4.37 (br s, 2H, piperazine-H), 4.57 (s, 2H, CH_2S), 6.97 (t, J = 7.2 Hz, 1H, Ph 4′-H), 7.0 (d, J = 7.2 Hz, 1H, Ph 6′-H), 7.13 (t, J = 7.2 Hz, 1H, Ph 5′-H), 7.16 (d, J = 7.2 Hz, 1H, Ph 3′-H), 7.33 (d, J = 8.4 Hz, 1H, quinazoline 8-H), 7.73 (d, J = 8.4 Hz, 1H, quinazoline 7-H), 8.22 (s, 1H, quinazoline 5-H), 8.43 (br s, 2H, NH_2). ESI-MS m/z: 425 $[M + H]^+$. ESI-HRMS m/z: calcd for $C_{21}H_{25}N_6S_2$ ($[M + H]^+$): 425.1582, found: 425.1567.

*6.1.7.9. (2,4-Diaminoquinazolin-6-yl)methyl 4-(2,4-dimethylphenyl) piperazine-1-carbodithioate (**8i**).* Yield 54%, white solid, mp 211.2–212.8 °C (CC, eluent:dichloromethane/methanol = 90:10). ^{1}H NMR (600 MHz, DMSO-d_6) δ: 2.20 (s, 3H, CH_3), 2.24 (s, 3H, CH_3), 2.87 (br s, 4H, piperazine-H), 4.03 (br s, 2H, piperazine-H), 4.38 (br s, 2H, piperazine-H), 4.53 (s, 2H, CH_2S), 6.42 (br s, 2H, NH_2), 6.91 (d, J = 8.4 Hz, 1H, Ph 6′-H), 6.94 (d, J = 8.4 Hz, 1H, Ph 5′-H), 6.99 (s, 1H, Ph 3′-H), 7.21 (d, J = 8.4 Hz, 1H, quinazoline 8-H), 7.58 (d, J = 8.4 Hz, 1H, quinazoline 7-H), 7.62 (br s, 2H, NH_2), 8.06 (s, 1H, quinazoline 5-H). ESI-MS m/z: 439 $[M + H]^+$. ESI-HRMS m/z: calcd for $C_{22}H_{27}N_6S_2$ ($[M + H]^+$): 439.1739, found: 439.1728.

*6.1.7.10. (2,4-Diaminoquinazolin-6-yl)methyl 4-(4-chlorophenyl) piperazine-1-carbodithioate (**8j**).* Yield 35%, white solid, mp 206.6–208.0 °C (CC, eluent:dichloromethane/methanol = 90:10). ^{1}H NMR (300 MHz, DMSO-d_6) δ: 3.43 (br s, 4H, piperazine-H), 4.07 (br s, 2H, piperazine-H), 4.41 (br s, 2H, piperazine-H), 4.56 (s, 2H, CH_2S), 6.98 (d, J = 9.0 Hz, 2H, Ph 2′ and 6′-H), 7.23 (d, J = 8.7 Hz, 1H, quinazoline 8-H), 7.29 (d, J = 9.0 Hz, 2H, Ph 3′ and 5′-H), 7.60 (dd, J = 8.7, 1.5 Hz, 1H, quinazoline 7-H), 8.09 (d, J = 1.5 Hz, 1H, quinazoline 5-H). ESI-MS m/z: 445 $[M + H]^+$. ESI-HRMS m/z: calcd for $C_{20}H_{22}ClN_6S_2$ ($[M + H]^+$): 445.1036, found: 445.1028.

*6.1.7.11. (2,4-Diaminoquinazolin-6-yl)methyl 4-(2-chlorophenyl) piperazine-1-carbodithioate (**8k**).* Yield 41%, white solid, mp 245.1–246.1 °C (CC, eluent:dichloromethane/methanol = 90:10). ^{1}H NMR (300 MHz, DMSO-d_6) δ: 3.09 (br s, 4H, piperazine-H), 4.07 (br s, 2H, piperazine-H), 4.40 (br s, 2H, piperazine-H), 4.59 (s, 2H, CH_2S), 7.10 (td, J = 7.8, 1.2 Hz, 1H, Ph 4′-H), 7.20 (dd, J = 7.8, 1.2 Hz, 1H, Ph 6′-H), 7.33 (td, J = 7.8, 1.2 Hz, 1H, Ph 5′-H), 7.35 (d, J = 8.4 Hz, 1H, quinazoline 8-H), 7.46 (dd, J = 7.8, 1.2 Hz, 1H, Ph 3′-H), 7.75 (d, J = 8.4 Hz, 1H, quinazoline 7-H), 8.22 (s, 1H, quinazoline 5-H), 8.39 (br s, 2H, NH_2). ESI-MS m/z: 445 $[M + H]^+$. ESI-HRMS m/z: calcd for $C_{20}H_{22}ClN_6S_2$ ($[M + H]^+$): 445.1036, found: 445.1032.

*6.1.7.12. (2,4-Diaminoquinazolin-6-yl)methyl 4-(3,4-dichlorophenyl) piperazine-1-carbodithioate (**8l**).* Yield 27%, grey solid, mp 233.6–236.4 °C (CC, eluent:dichloromethane/methanol = 90:10). ^{1}H NMR (300 MHz, DMSO-d_6) δ: 3.18 (br s, 4H, piperazine-H), 4.07 (br s, 2H, piperazine-H), 4.36 (br s, 2H, piperazine-H), 4.56 (s, 2H, CH_2S), 6.80 (br s, 2H, NH_2), 6.93 (dd, J = 9.0, 3.0 Hz, 1H, Ph 6′-H), 7.15 (d, J = 3.0 Hz, 1H, Ph 2′-H), 7.27 (d, J = 8.4 Hz, 1H, quinazoline 8-H), 7.44 (d, J = 9.0 Hz, 1H, Ph 5′-H), 7.65 (d, J = 8.4 Hz, 1H, quinazoline 7-H), 7.97 (br s, 2H, NH_2), 8.13 (s, 1H, quinazoline 5-H). ESI-MS m/z: 479 $[M + H]^+$. ESI-HRMS m/z: calcd for $C_{20}H_{21}Cl_2N_6S_2$ ($[M + H]^+$): 479.0646, found: 479.0638.

*6.1.7.13. (2,4-Diaminoquinazolin-6-yl)methyl 4-(4-fluorophenyl) piperazine-1-carbodithioate (**8m**).* Yield 87%, white solid, mp 249.0–349.8 °C (CC, eluent:dichloromethane/methanol = 80:20). ^{1}H NMR (200 MHz, DMSO-d_6) δ: 3.21 (br s, 4H, piperazine-H), 4.06 (br s, 2H, piperazine-H), 4.37 (br s, 2H, piperazine-H), 4.58 (s, 2H, CH_2S), 6.94–7.13 (m, 4H, Ph-H), 7.32 (d, J = 8.4 Hz, 1H, quinazoline 8-H), 7.72 (d, J = 8.4 Hz, 1H, quinazoline 7-H), 8.16 (s, 1H, quinazoline 5-H). ESI-MS m/z: 429 $[M + H]^+$. Anal. calcd. for $C_{20}H_{21}FN_6S_2 \cdot 1/2H_2O$: C, 54.90; H, 5.07; N, 19.21. Found: C, 54.90; H, 5.03; N, 18.95.

*6.1.7.14. (2,4-Diaminoquinazolin-6-yl)methyl 4-(2-fluorophenyl) piperazine-1-carbodithioate (**8n**).* Yield 73%, white solid, mp 232.3–234.3 °C (CC, eluent:dichloromethane/methanol = 90:10). ^{1}H NMR (600 MHz, DMSO-d_6) δ: 3.10 (br s, 4H, piperazine-H), 4.05 (br s, 2H, piperazine-H), 4.39 (br s, 2H, piperazine-H), 4.51 (s, 2H, CH_2S), 6.27 (br s, 2H, NH_2), 6.99 (m, 1H, Ph 4′-H), 7.04 (t, J = 8.4 Hz, 1H, Ph 6′-H), 7.10 (t, J = 8.4 Hz, 1H, Ph 5′-H), 7.46 (m, 1H, Ph 3′-H), 7.35 (d, J = 8.4 Hz, 1H, quinazoline 8-H), 7.49 (br s, 2H, NH_2), 7.56 (d, J = 8.4 Hz, quinazoline 7-H), 8.03 (s, 1H, quinazoline 5-H). ESI-MS m/z: 429 $[M + H]^+$. ESI-HRMS m/z: calcd for $C_{20}H_{22}FN_6S_2$ ($[M + H]^+$): 429.1331, found: 429.1325.

*6.1.7.15. (2,4-Diaminoquinazolin-6-yl)methyl 4-(2,4-difluorophenyl) piperazine-1-carbodithioate (**8o**).* Yield 44%, white solid, mp > 300 °C (CC, eluent:dichloromethane/methanol = 90:10). ^{1}H NMR (300 MHz, DMSO-d_6) δ: 3.06 (br s, 4H, piperazine-H), 4.05 (br s, 2H, piperazine-H), 4.39 (br s, 2H, piperazine-H), 4.54 (s, 2H, CH_2S), 6.80 (br s, 2H, NH_2), 7.02 (td, J = 8.4, 1.2 Hz, 1H, Ph 3′-H), 7.10 (m, 1H, Ph 6′-H), 7.22 (m, 2H, Ph 5′-H and quinazoline 8-H), 7.63 (dd, J = 8.4, 2.4 Hz, 1H, quinazoline 7-H), 7.90 (m, 2H, NH_2), 8.12 (d, J = 2.4 Hz, 1H, quinazoline 5-H). ESI-MS m/z: 447 $[M + H]^+$. ESI-HRMS m/z: calcd for $C_{20}H_{21}F_2N_6S_2$ ($[M + H]^+$): 447.1237, found: 447.1235.

*6.1.7.16. (2,4-Diaminoquinazolin-6-yl)methyl 4-(4-acetylphenyl)piperazine-1-carbodithioate (**8p**).* Yield 33%, yellow solid, mp > 300 °C (from DMF/acetone). ^{1}H NMR (300 MHz, DMSO-d_6) δ: 2.46 (s, 3H, $COCH_3$), 3.56 (br s, 4H, piperazine-H), 4.06 (br s, 2H, piperazine-H), 4.38 (br s, 2H, piperazine-H), 4.52 (s, 2H, CH_2S), 6.01 (br s, 2H, NH_2), 6.93 (d, J = 9.0 Hz, 2H, Ph 2′ and 6′-H), 7.14 (d, J = 8.4 Hz, 1H, quinazoline 8-H), 7.26 (br s, 2H, NH_2), 7.51 (d, J = 8.4 Hz, 1H, quinazoline 7-H), 7.83 (d, J = 9.0 Hz, 2H, Ph 3′ and 5′-H), 7.96 (s, 1H, quinazoline 5-H). ESI-MS m/z: 453 $[M + H]^+$. ESI-HRMS m/z: calcd for $C_{22}H_{25}N_6OS_2$ ($[M + H]^+$): 453.1531, found: 453.1533.

*6.1.7.17. (2,4-Diaminoquinazolin-6-yl)methyl 4-(4-nitrophenyl)piperazine-1-carbodithioate (**8q**).* Yield 28%, yellow solid, mp > 300 °C (from DMF/acetone). ^{1}H NMR (300 MHz, DMSO-d_6) δ: 3.69 (br s, 4H, piperazine-H), 4.08 (br s, 2H, piperazine-H), 4.37 (br s, 2H, piperazine-H), 4.51 (s, 2H, CH_2S), 5.99 (br s, 2H, NH_2), 6.93 (d, J = 9.6 Hz, 2H, Ph 2′ and 6′-H), 7.13 (d, J = 8.4 Hz, 1H, quinazoline 8-H), 7.24 (br s, 2H, NH_2), 7.50 (dd, J = 8.4, 1.8 Hz, 1H, quinazoline 7-H), 7.99 (d, J = 1.8 Hz, 1H, quinazoline 5-H), 8.09 (d, J = 9.6 Hz, 2H, Ph 3′ and 5′-H). ESI-MS m/z: 456 $[M + H]^+$. ESI-HRMS m/z: calcd for $C_{20}H_{22}N_7O_2S_2$ ($[M + H]^+$): 456.1276, found: 456.1273.

*6.1.7.18. (2,4-Diaminoquinazolin-6-yl)methyl 4-(2-nitrophenyl)piperazine-1-carbodithioate (**8r**).* Yield 24%, yellow solid, mp > 300 °C (CC, eluent:dichloromethane/methanol = 90:10). ^{1}H NMR (600 MHz, DMSO-d_6) δ: 3.15 (br s, 4H, piperazine-H), 4.02 (br s, 2H, piperazine-H), 4.32 (br s, 2H, piperazine-H), 4.57 (s, 2H, CH_2S), 6.65 (br s, 2H, NH_2), 7.15 (t, J = 7.8 Hz, 1H, Ph 4′-H), 7.23 (d, J = 8.4 Hz, 1H, quinazoline 8-H), 7.33 (m, 2H, NH_2), 7.59 (t, J = 7.8 Hz, 1H, Ph 5′-H), 7.71 (d, J = 8.4 Hz, 1H, quinazoline 7-H), 7.84 (d, J = 7.8 Hz, 1H, Ph 6′-H), 7.89 (d, J = 7.8 Hz, 1H, Ph 3′-H), 8.18 (s, 1H, quinazoline 5-H). ESI-MS m/z: 456 $[M + H]^+$. ESI-HRMS m/z: calcd for $C_{20}H_{22}N_7O_2S_2$ ($[M + H]^+$): 456.1276, found: 456.1272.

*6.1.7.19. (2,4-Diaminoquinazolin-6-yl)methyl 4-(4-(trifluoromethyl) phenyl)piperazine-1-carbodithioate (**8s**).* Yield 43%, mp 263.0–264.0 °C (CC, eluent:dichloromethane/methanol = 90:10). ^{1}H NMR (600 MHz, DMSO-d_6) δ: 3.47 (br s, 4H, piperazine-H), 4.04 (br s, 2H, piperazine-H), 4.36 (br s, 2H, piperazine-H), 4.56 (s, 2H, CH_2S), 7.01 (d, J = 8.4 Hz, 2H, Ph 2′ and 6′-H), 7.11 (m, 2H, NH_2), 7.29 (d, J = 8.4 Hz, 1H, quinazoline 8-H), 7.51 (d, J = 8.4 Hz, 2H, Ph 3′ and

5′-H), 7.54 (m, 2H, NH_2), 7.68 (d, J = 8.4 Hz, 1H, quinazoline 7-H), 8.17 (s, 1H, quinazoline 5-H). ESI-MS m/z: 479 $[M + H]^+$. ESI-HRMS m/z: calcd for $C_{21}H_{22}F_3N_6S_2$ ($[M + H]^+$): 479.1299, found: 479.1298.

*6.1.7.20. (2,4-Diaminoquinazolin-6-yl)methyl 4-(pyridin-2-yl)piperazine-1-carbodithioate (**8t**).* Yield 62%, white solid, mp 238.3–238.8 °C (CC, eluent:dichloromethane/methanol = 90:10). ^{1}H NMR (300 MHz, DMSO-d_6) δ: 3.65 (br s, 4H, piperazine-H), 4.01 (br s, 2H, piperazine-H), 4.34 (br s, 2H, piperazine-H), 4.52 (s, 2H, CH_2S), 6.40 (br s, 2H, NH_2), 6.67 (t, J = 7.2 Hz, 1H, pyridine 5′-H), 6.81 (d, J = 7.2 Hz, 1H, pyridine 3′-H), 7.19 (d, J = 8.4 Hz, 1H, quinazoline 8-H), 7.58 (m, 4H, quinazoline 7-H, pyridine 4′-H and NH_2), 8.06 (s, 1H, quinazoline 5-H), 8.12 (dd, J = 7.2, 1.8 Hz, 1H, pyridine 6′-H). ESI-MS m/z: 412 $[M + H]^+$. ESI-HRMS m/z: calcd for $C_{19}H_{22}N_7S_2$ ($[M + H]^+$): 412.1378, found: 412.1375.

*6.1.7.21. (2,4-Diaminoquinazolin-6-yl)methyl 4-(pyrimidin-2-yl)piperazine-1-carbodithioate (**8u**).* Yield 35%, white solid, mp 246.2–247.5 °C (CC, eluent:dichloromethane/methanol = 90:10). ^{1}H NMR (300 MHz, DMSO-d_6) δ: 3.86 (br s, 4H, piperazine-H), 4.01 (br s, 2H, piperazine-H), 4.33 (br s, 2H, piperazine-H), 4.51 (s, 2H, CH_2S), 6.30 (br s, 2H, NH_2), 6.68 (t, J = 4.8 Hz, 1H, pyrimidine 5′-H), 7.17 (d, J = 8.7 Hz, 1H, quinazoline 8-H), 7.52 (br s, 2H, NH_2), 7.55 (dd, J = 8.7, 1.8 Hz, 1H, quinazoline 7-H), 8.04 (d, J = 1.8 Hz, 1H, quinazoline 5-H), 8.38 (d, J = 4.8 Hz, 2H, pyrimidine 4′ and 6′-H). ESI-MS m/z: 413 $[M + H]^+$. ESI-HRMS m/z: calcd for $C_{18}H_{21}N_8S_2$ ($[M + H]^+$): 413.1331, found: 413.1322.

6.2. MTT assay

Antiproliferative activity of the synthesized compounds was determined by the MTT assay on the following cell lines: A549, MCF-7, HeLa, HT29 and HCT-116. All cancer cells were grown in high glucose DMEM supplemented with 10% fetal bovine serum, 2 mM glutamine, 50 units/mL penicillin, and 50 mg/mL streptomycin. Cell proliferation assay was performed using the CellTiter 96® AQ_{ueous} One Solution Cell Proliferation Assay (Promega). The tested compounds were prepared in DMSO as stock solutions and stored at −20 °C. After thawing, the stock solutions were freshly diluted to a series of concentrations in medium just prior to the assay. Final concentration of DMSO in medium was 0.2%.

Cells in logarithmic growth were plated in 96-well plate at following densities: 7.5×10^3 cells/well for A549, 5×10^3 cells/well for MCF-7, 1×10^4 cells/well for HeLa, 5×10^3 cells/well for HT29, and 5×10^3 cells/well for HCT-116. 24 h after seeding, 10 μL of 2% DMSO (vehicle control) or solution of the tested compounds was added into each well and incubated for 72 h, 20 μL of MTT solution was then added into each well and incubated for additional 2 h, and absorbance at 492 nm was measured on a microplate reader. Cell proliferation inhibition was given by the expression:

$$\text{Cell proliferation inhibition (\%)} = \left[1 - \left(OD_{\text{cells+test compound}} - OD_{\text{blank}}\right) \Big/ \left(OD_{\text{cells+DMSO}} - OD_{\text{blank}}\right)\right] \times 100\%$$

where OD means the absorbance at 492 nm in the test ($OD_{\text{cells + test compound}}$), control ($OD_{\text{cells + DMSO}}$) or blank ($OD_{\text{blank}}$) wells. Each value was the means of three independent experiments. The concentration causing 50% proliferation inhibition (IC_{50}) was determined from the sigmoidal curve obtained by plotting percent cell proliferation inhibition versus concentration using SPSS 16.0 for Windows. 5-Fluorouracil, a positive control, was tested in the same way.

6.3. Dihydrofolate reductase (DHFR) inhibition assay

The DHFR inhibition assay was performed using the DHFR assay kit (Sigma, CS0340). Briefly, the assay mixture contained 60 μM NADPH, 0.015 unit human DHFR, 5 μL DMSO or the same volume of DMSO solution containing one test compound to a specific final concentration, and DHFR assay buffer (950 μM $Na_2HPO_4 \cdot 7H_2O$, 134 μM KH_2PO_4 and 100 μM KCl, pH 7.5), in a final volume of 1.0 mL. After addition of the enzyme, the mixture was incubated at room temperature for 2.0 min, and the reaction was initiated by adding 50 μM dihydrofolate. The change in absorbance (ΔOD) was measured at 340 nm for 2.5 min under 22 °C. Results were reported as % inhibition of enzymatic activity calculated using the following formula:

$$\%\ \text{inhibition} = \left(1 - \Delta OD_{\text{test compound}} / \Delta OD_{\text{DMSO}}\right) \times 100\%$$

Each assay was independently performed three times and the means was determined. The 50% inhibitory concentration (IC_{50}) of each test compound was determined from the sigmoidal curve obtained by plotting the % inhibition values versus concentrations using SPSS 16.0 for Windows.

6.4. Thymidylate synthase (TS) inhibition assay

The coding region of human TS was amplified by reverse-transcription PCR from mRNA extracted from HeLa cells and was subcloned into XhoI and KpnI sites in pTrcHis vector (Invitrogen). The resulting expression construct pTrcHis-TS was transformed into the bacterial strain Rosetta (DE3), and its expression was induced with IPTG. The recombinant His-TS was purified using Nickle resin (Qiagen). The purity of His-TS was examined by SDS-PAGE. The purified enzymes were stored at −80 °C in PBS with 10% glycerol. Enzyme activity was determined spectrophotometrically by the increasing absorbance at 340 nm due to the oxidation reaction of N^5,N^{10}-methylenetetrahydrofolate to dihydrofolate. The standard assay buffer was prepared with 50 mM TES *N*-tris(hydroxymethyl)methyl-2-aminoethanesulfonic acid at pH 7.4, 25 mM $MgCl_2$, 6.5 mM formaldehyde, 1 mM EDTA, and 75 mM 2-mercaptoethanol. A reaction solution was assembled by mixing 120 μM dUMP, 140 μM 6(*R*,*S*)-1-CH_2CH_4-folate, 0.07 μM TS enzyme, and varying concentrations of synthesized compounds or RTX (a positive control) in the standard assay buffer. Assays were performed at 20 °C for 20 min and OD at 340 nm was determined using a UV spectrophotometry. The net change of OD at 340 nm in the sample in the presence of TS only, $\Delta OD_{\text{control}}$, served as the base, while the net change of OD at 340 nm in the sample in the presence of both TS and tested compound was recorded as $\Delta OD_{\text{test compound}}$. The percentage of inhibition was calculated as $(1 - \Delta OD_{\text{test compound}}/\Delta OD_{\text{control}}) \times 100\%$.

Each assay was independently performed three times and the means was determined. The 50% inhibitory concentration (IC_{50}) of each test compound was determined from the sigmoidal curve obtained by plotting the % inhibition values versus concentrations using SPSS 16.0 for Windows.

6.5. Determination of the cell cycle profiles and mitotic index

Cell cycle profiles were determined by propidium iodide staining and fluorescence-activated cell sorter analysis. Mitotic index was determined essentially as described previously [23].

Phospho-Histone H3 (Ser-10) rabbit polyclonal antibodies were purchased from Bethyl Laboratories, Inc.

6.6. Indirect immunofluorescence assay

Indirect immunofluorescence assay was performed as described before [24,25]. Monoclonal antibody against γ-H2AX (clone JBW301) was purchased from Millipore and used in a dilution of 1:1500.

Acknowledgements

This work was supported by National Natural Science Foundation of China (Project No. 20972099 and 31130017), Beijing Municipal Commission of Education (Project No. KZ201210028035), the 973 Project 2013CB911000, and the Funding Project for Academic Human Resources Development in Institutions of Higher Learning Under the Jurisdiction of Beijing Municipality (PHR20110508).

References

[1] A.L. Jackman, F.T. Boyle, K.R. Harrap, Tomudex (ZD1694), from concept to care, a program in rational drug discovery, Invest. New Drugs 14 (1996) 305–316.
[2] D. Cunningham, J. Zalcberg, J. Maroun, R. James, S. Clarke, T.S. Maughan, M. Vincent, J. Schulz, M.G. Baron, T. Facchini, Efficacy, tolerability and management of raltitrexed (Tomudex™) monotherapy in patients with advanced colorectal cancer: a review of phase II/III trials, Eur. J. Cancer 38 (2002) 478–486.
[3] S.E. Webber, T.M. Bleckman, J. Attard, J.G. Deal, V. Katherdekar, K.M. Welsh, S. Webber, C.A. Janson, D.A. Matthews, W.W. Smith, S.T. Freer, S.R. Jordan, R.J. Bacquet, E.F. Howland, C.J.L. Booth, R.W. Ward, S.M. Hermann, J. White, C.A. Morse, J.A. Hilliard, C.A. Bartlett, Design of thymidylate synthase inhibitors using protein crystal structures: the synthesis and biological evaluation of a novel class of 5-substituted quinazolines, J. Med. Chem. 36 (1993) 733–746.
[4] S. Webber, C.A. Bartlett, T.J. Boritzki, J.A. Hilliard, E.F. Howland, A.L. Johnston, M. Kosa, S.A. Margosiak, C.A. Morse, B.V. Shetty, AG337, a novel lipophilic thymidylate synthase inhibitor: *in vitro* and in vivo preclinical studies, Cancer Chemother. Pharmacol. 37 (1996) 509–517.
[5] A. Gangjee, W. Li, J. Yang, R.L. Kisliuk, Design, synthesis, and biological evaluation of classical and nonclassical 2-amino-4-oxo-5-substituted-6-methylpyrrolo[3,2-*d*]pyrimidines as dual thymidylate synthase and dihydrofolate reductase inhibitors, J. Med. Chem. 51 (2008) 68–76.
[6] A. Gangjee, X. Lin, R.L. Kisliuk, J.J. McGuire, Synthesis of *N*-{4-[(2,4-diamino-5-methyl-4,7-dihydro-3*H*-pyrrolo[2,3-*d*]pyrimidin-6-yl)thio]benzoyl}-L-glutamic acid and *N*-{4-[(2-Amino-4-oxo-5-methyl-4,7-dihydro-3*H*-pyrrolo[2,3-*d*]pyrimidin-6-yl)thio]benzoyl}-L-glutamic acid as dual inhibitors of dihydrofolate reductase and thymidylate synthase and as potential antitumor agents, J. Med. Chem. 48 (2005) 7215–7222.
[7] A. Gangjee, H.D. Jain, S. Kurup, Recent advances in classical and non-classical antifolates as antitumor and antiopportunistic infection agents: part I, Anti-Cancer Agents Med. Chem. 7 (2007) 524–542.
[8] A. Gangjee, H.D. Jain, S. Kurup, Recent advances in classical and non-classical antifolates as antitumor and antiopportunistic infection agents: part II, Anti-Cancer Agents Med. Chem. 8 (2008) 205–231.
[9] A. Ciccia, S.J. Elledge, The DNA damage response: making it safe to play with knives, Mol. Cell. 40 (2010) 179–204.
[10] M. Pilátová, M. Šarišský, P. Kutschy, A. Miroššay, R. Mezencev, Z. Čurillová, M. Suchý, K. Monde, L. Mirossay, J. Mojžiš, Cruciferous phytoalexins: antiproliferative effects in T-Jurkat leukemic cells, Leuk. Res. 29 (2005) 415–421.
[11] P. Csomós, I. Zupkó, B. Réthy, L. Fodor, G. Falkay, G. Bernáth, Isobrassinin and its analogues: novel types of antiproliferative agents, Bioorg. Med. Chem. Lett. 16 (2006) 6273–6276.
[12] X. Hou, Z. Ge, T. Wang, W. Guo, J. Cui, T. Cheng, C. Lai, R. Li, Dithiocarbamic acid esters as anticancer agent. Part 1: 4-substituted-piperazine-1-carbodithioic acid 3-cyano-3,3-diphenyl-propyl esters, Bioorg. Med. Chem. Lett. 16 (2006) 4214–4219.
[13] M.A.-H. Zahran, T.A.-R. Salem, R.M. Samaka, H.S. Agwa, A.R. Awad, Design, synthesis and antitumor evaluation of novel thalidomide dithiocarbamate and dithioate analogs against Ehrlich ascites carcinoma-induced solid tumor in Swiss albino mice, Bioorg. Med. Chem. 16 (2008) 9708–9718.
[14] P. Gaspari, T. Banerjee, W.P. Malachowski, A.J. Muller, G.C. Prendergast, J. DuHadaway, S. Bennett, A.M. Donovan, Structure–activity study of brassinin derivatives as indoleamine 2,3-dioxygenase inhibitors, J. Med. Chem. 49 (2006) 684–692.
[15] S.L. Cao, Y.P. Feng, Y.Y. Jiang, S.Y. Liu, G.Y. Ding, R.T. Li, Synthesis and *in vitro* antitumor activity of 4(3*H*)-quinazolinone derivatives with dithiocarbamate side chains, Bioorg. Med. Chem. Lett. 15 (2005) 1915–1917.
[16] S.L. Cao, Y.P. Feng, X.L. Zheng, Y.Y. Jiang, M. Zhang, Y. Wang, M. Xu, Synthesis of substituted-benzylamino- and heterocyclylmethylamino-carbodithioate derivatives of 4(3*H*)-quinazolinone and their cytotoxic activity, Arch. Pharm. 339 (2006) 250–254.
[17] S.L. Cao, Y. Wang, L. Zhu, J. Liao, Y.W. Guo, L.L. Chen, H.Q. Liu, X. Xu, Synthesis and cytotoxic activity of *N*-((2-methyl-4(3*H*)-quinazolinon-6-yl)methyl)dithiocarbamates, Eur. J. Med. Chem. 45 (2010) 3850–3857.
[18] G.R. Bedford, M.W. Partridge, A convenient preparation of *o*-aminoaryl cyanides, J. Chem. Soc. (1959) 1633–1634.
[19] N.S.A. Zeni, Preparation of *o*-cyanoanilines from Isatin Oximes. JP 2003064039A (2003).
[20] L.M. Werbel, E.F. Elslager, L.S. Newton, Antimalarial agents. Part 62. Synthesis and antimalarial activity of a series of 2,4-diamino-6-[(*N*-alkylanilino)methyl] quinazolines, J. Heterocycl. Chem. 24 (1987) 345–349.
[21] I.D. Goldman, S. Chattopadhyay, R. Zhao, R. Moran, The antifolates: evolution, new agents in the clinic, and how targeting delivery via specific membrane transporters is driving the development of a next generation of folate analogs, Curr. Opin. Investig. Drugs 11 (2010) 1409–1423.
[22] A.P. Stankevicius, P.B. Terentiev, L.N. Janushene1, A.B. Savickas, Chem. Heterocycl. Compd. 41 (2005) 98–104.
[23] X. Xu, J.H. Lee, D.F. Stern, Microcephalin is a DNA damage response protein involved in regulation of CHK1 and BRCA1, J. Biol. Chem. 279 (2004) 34091–34094.
[24] X. Xu, D.F. Stern, NFBD1/MDC1 regulates ionizing radiation-induced focus formation of DNA checkpoint signaling and repair factors, FASEB J. 17 (2003) 1842–1848.
[25] X. Xu, D.F. Stern, NFBD1/KIAA0170 is a chromatin-associated protein involved in DNA damage signaling pathways, J. Biol. Chem. 278 (2003) 8795–8803.